Zinc-binding properties of Junín virus nucleocapsid protein

M. Alejandra Tortorici,[1] P. Daniel Ghiringhelli,[2] Mario E. Lozano,[2] César G. Albariño[1]†
and Víctor Romanowski[1,2]

[1] Instituto de Bioquímica y Biología Molecular, Depto de Ciencias Biológicas, Facultad de Ciencias Exactas, Universidad Nacional de La Plata, Calles 47 y 115, 1900 La Plata, Buenos Aires, Argentina

[2] Laboratorio de Ingeniería Genética y Biología Celular y Molecular, Departamento de Ciencia y Tecnología, Centro de Estudios e Investigaciones, Universidad Nacional de Quilmes, Roque Saenz Peña 180, 1876 Bernal, Buenos Aires, Argentina

The arenavirus nucleocapsid protein (N) is a highly basic 63 kDa protein with a dual function during the virus life-cycle. First, it is involved in essential steps of genome replication, promoting the synthesis of the full-length antigenomic copy of S RNA, and second it associates with the genomic RNA to form the nucleocapsid. We have expressed the N protein of Junín virus in *E. coli* and shown that it binds zinc *in vitro*. This property is in agreement with the presence in the carboxy-terminal region of the N protein of the $CX_2HX_{23}CX_4C$ sequence, which resembles a classical zinc-finger motif. The specificity for zinc binding was demonstrated by competition with other divalent metal ions. The ability of the predicted motif to bind zinc was established by analysis of a series of N mutants, including truncated variants and amino acid substitutions. In addition, alternative zinc-binding sites were found.

Introduction

Arenaviruses are enveloped viruses with a genome composed of two single-stranded RNA species, designated L (large, ca. 7 kb) and S (small, ca. 3·5 kb). Junín virus, a South American arenavirus, is the aetiological agent of a severe endemo-epidemic disease called Argentine haemorrhagic fever. The complete nucleotide sequence of the S RNA of Junín virus has been determined for different strains (Ghiringhelli *et al.*, 1991, 1997; Albariño *et al.*, 1997, 1998). The S RNA encodes the major structural proteins of the virion, which are the precursor of the envelope glycoproteins (GPC) and the viral nucleocapsid protein (N). Open reading frames are arranged in opposite orientations (ambisense coding strategy; Auperin *et al.*, 1984) and are separated by a non-coding intergenic region that folds into a stable stem–loop secondary structure (Ghiringhelli *et al.*, 1991). Once the virus enters a cell, the genomic form of the S RNA is transcribed and yields only two antigenic forms: the 1·8 kb N mRNA and a 3·4 kb full-length antigenomic S RNA. The N mRNA is the first RNA species to be transcribed in the infected cell, and the structure of the intergenic region seems to be the transcriptional termination signal (Franze-Fernández *et al.*, 1993; Tortorici *et al.*, 2000). The N protein is a highly basic protein, translated from an antigenomic sense mRNA species that is encoded in the 3′ half of the viral S RNA (Romanowski, 1993). N displays a dual function during the viral life-cycle: it associates tightly with the genomic RNA to form the nucleocapsids and, as recently demonstrated, it is essential for genome replication, since it promotes the synthesis of the genomic replicative form in the viral life-cycle (Lee *et al.*, 2000; Tortorici *et al.*, 2000).

In general, RNA–protein interactions involve both specific and non-specific contacts and a number of protein sequences and/or structural motifs have evolved to allow such interaction. Among these motifs are the classical zinc fingers or the general RING fingers, which are autonomously folding domains that require zinc for proper folding and RNA-binding activity (Nolte *et al.*, 1998; McColl *et al.*, 1999). We found one classical zinc-finger domain near the carboxyl terminus of the N protein sequence (Parisi *et al.*, 1996). In this work we demonstrate that N protein binds zinc specifically. Furthermore, we analysed a series of mutant N proteins to characterize the zinc-binding region. The experimental results demonstrate that the zinc-binding activity is located at the carboxy-terminal region of the N protein and that the substitution of critical amino acid residues eliminates binding in the isolated zinc finger, but alternative binding sites located in the immediately adjacent or partially overlapping region, may bind Zn^{2+} with a slightly lower affinity.

Author for correspondence: Victor Romanowski (at address 1).
Fax +54 221 4259223. e-mail victor@biol.unlp.edu.ar

† **Present address:** Department of Microbiology, University of Alabama at Birmingham, Birmingham, AL 35294, USA.

Methods

■ **Molecular cloning and oligonucleotides.** Plasmids were propagated in *E. coli* DH5α grown in Luria–Bertani broth. Standard procedures were used for DNA manipulations (Sambrook *et al.*, 1989) according to manufacturers' protocols. All DNA oligomers are listed in Table 1, as are the positions of the nucleotide sequences used to obtain the mutant proteins (translation initiation codon, translation stop codon and amino acid substitutions).

■ **Sequence alignments.** Alignment of arenavirus N protein sequences was done using the Clustal X program (Thompson *et al.*, 1997) and the substitution matrix PAM 250. The parameters used for the pairwise and multiple alignment were GAP opening = 10, GAP extension = 0·1 and GAP opening = 10, GAP extension = 0·05, respectively.

■ **Construction of deletion and substitution mutants of N gene.** Plasmid pBJUNS (Ghiringhelli *et al.*, 1991) containing the entire N ORF of Junín virus (strain MC2) was the progenitor of plasmids used in this work. The N ORF was amplified by PCR using primers N1 and N2 (Table 1). The PCR product was inserted into pGEM-T (Promega). The N gene was recovered by digestion with *Nco*I and *Bam*HI, filled-in using the Klenow fragment of DNA polymerase I, and inserted by ligation into the filled-in *Nde*I site of pET-22b(+) under the control of a bacteriophage T7 promoter (Novagen). The putative zinc-finger domain was generated by PCR using primers ZfD and N2 (Table 1). The PCR product was ligated to pET-22b(+) vector following the same strategy used for the N ORF. Mutations which resulted in carboxy-terminal deletions of the N ORF were made using the Erase-a-Base System (Promega). ExoIII/S1 deleted products containing the authentic methionine codon of the N protein were modified to include stop codons immediately after the last N amino acid. To this end, oligonucleotides ST1 and ST2 (see Table 1) were designed to incorporate stop codons in each of the open reading frames. The oligonucleotide mixture (25 µM each) was heated at 100 °C for 5 min, annealed in 100 mM NaCl, 10 mM Tris–HCl pH 7·5, 0·1 mM EDTA and the ST1/ST2 heteroduplex ligated to the ExoIII products. The deleted genes were finally generated by PCR, using primers N1 and ST2, and the amplified fragments were inserted into the NdeI site of pET-22b(+). Mutations that resulted in amino acid substitutions in the N gene were introduced by site-directed PCR mutagenesis and PCR combinations of overlapping fragments using *Pfu* polymerase and the appropriate combinations of primers listed in Table 1 (Higuchi, 1989;

Table 1. DNA oligonucleotides used in the study

All the mutagenized codons are indicated in bold.

Name	Size (nt)	Sequence	Use and description
N1	30	AGATCTGGAT<u>CC**ATG**G</u>CACACTCCAAAGAG	5′ end primer used to generate N(1–564). The translational initiation codon is indicated in bold and the *Nco*I site is underlined.
N2	31	GAGATCT<u>GGATCC</u>**TTA**CAGTGCATAGGCTGC	3′ end primer used to generate N(1–564), N(478–564) and point mutant genes. The *Bam*HI site is underlined. The sequence complementary to the translational stop codon is indicated in bold.
ZfD*	28	GCATG<u>C**CATG**G</u>GAGAACAAGCCAGGCAG	5′ end primer used to generate N(478–564). Translation initiation codon is indicated in bold and the *Nco*I site is underlined. S to G conservative change was introduced to generate the *Nco*I site (mutagenized codon is boxed).
ST1	11	**TAA**T**TGA**T**TAG**	These complementary oligos were designed to incorporate stop codons (in bold) in the three open reading frames into the deletion mutant.
ST2†	15	GATCCTAATCAATTA	
ZfD(C525A)V	26	CTAGCAGAGC**AGC**GTGTGGCTCACTG	5′ end primer used to generate a mutant with the $C^{525} \rightarrow A$ substitution.
ZfD(C530A)V	31	ACACTGACTGAAACATTAT**GGC**GTCTAGCAG	5′ end primer used to introduce a $C^{530} \rightarrow A$ substitution.
ZfD(C497A; H500N)V	29	ACTCCATT**GTT**ATGTTT**GGC**TAGGTGGCC	5′ end primer used to introduce the $C^{497} \rightarrow A$ substitution and the $H^{500} \rightarrow N$ substitution.
ZfD(C525A)VC	26	CAGTGAGCCACACG**CTG**CTCTGCTAG	3′ end primer used to introduce a $C^{525} \rightarrow A$ substitution.
ZfD(C530A)VC	31	CTGCTAGAC**GCC**ATAATGTTTCAGTCAGTGT	3′ end primer used to introduce a $C^{530} \rightarrow A$ substitution.
ZfD(C497A; H500N)VC	29	GGCCACCTA**GCC**AAACAT**AAC**AATGGAGT	3′ end primer used to introduce the $C^{497} \rightarrow A$ substitution and the $H^{500} \rightarrow N$ substitution.

* ZfD, zinc-finger domain.
† ST1/ST2, three frame stop adapters.

```
                          ↓↓        ↓            ↓ ↓                                                                    ↓
Cons.JUN    FQPAG..YIHCFRKPHDEKGFKNGSRHSHGILMKDIEDAMPGVLSYVIGLLPPDMVVTTQGSDDIRKLFDLHGRRDLKLVDVRL

LAG         YQPSSGCYVHFFREPTDLKQFKQDAKYSHGIDVTDLFAAQPGLTSAVIEALPRNMVITCQGSEDIRKLLESQGRRDIKLIDITL
LAJ         YQPSSGCYIHFFREPTDLKQFKQDAKYSHGIDVTDLFATQPGLTSAVIDALPRNMVITCQGSDDIRKLLESQGRKDIKLIDIAL
LCA         FQPQNGQFIHFYREPVDQKQFKQDSKYSHGMDLADLFNAQPGLTSSVIGALPQGMVLSCQGSDDIRKLLDSQNRKDIKLIDVEM
LCE         FQPQNGQFIHFYREPTDQKQFKQDSKYSHGMDLADLFNAQAGLTSSVIGALPQGMVLSCQGSDDIRKLLDSQNRRDIKLIDVEM
MOP         YQPNNGQYIHFYREPTDIKQFKQDSKHSHGIDIQDLFSVQPGLTSAVIESLPKNMVLSCQGADDIRKLLDSQNRRDIKLIDVSM
CD1         FQPAGKQYIHCFRKPHDEKGFKNGSRHSHGILMKDIEDAMPGVLSYVIGLLPPDMVVTTQGSDDIRKLFDLHGRRDLKLVDVRL
MC2         FQPAGSKYIHCFRKPHDEKGFKNGSRHSHGILMKDIEDAMPGVLSYVIGLLPPDMVVTTQGSDDIRKLFDLHGRRDLKLVDVRL
MAC         YQPANKHYIHCFRKPHDEKGFKNGSRHSHGILMQDIEDAMPGVLSYVIGLLPPDMVITTQGSDDIRKLLDIHGRKDLKLVDVKL
OLI         YQPTTGYYIHCFRLPHDEKGFKNGSKYSHGILLRDIENARSGLLSRILIKLPSKLVLTCQGSDDIKKLMELNGRPDISTIDLSF
PIC         YQPDTGNYIHCYRFPHDEKSFKEQNKYSHGLLLKDLADAQPGLISSIIRHLPQNMVFTAQGSDDIIRLFEMHGRRDLKVLDVKL
SAB         YQPDTGNYILCYRKPHDEKGFKNGSHGMLLKDLESAQPGLLSYVIGLLPPNMVLTTQGSDDINRLVDTHGRKDLKIVDIKL
TAC         YQPAKKQYIHCFRKPHDEKGFKNGSRHSHGILMKDIEDAVPGVLSYVIGLLPPNMVITTQGSDDIRKLLDIHGRKDLKIDVKF


                             ↓     ↓                            ↓
Cons. JUN   TSEQARQFDQQVWEKFGHLCKHHNGVVVSKKKRDKDAPFKLASSEPHCALLDCIMFQSVLDGKL-YEEELTPLLPPSLLFLPKAAYA-L

LAG         SKADSRKFENAVWDQFKDLCHMHTGVVVEKKKRGGKEE-----ITPHCALMDCIMFDAAVSGGL-DAKVLRVVLPRDMVFRTSTPKVVL
LAJ         SKTDSRKYENAVWDQYKDLCHMHTGVVVEKKKRGGKEE-----ITPHCALMDCIMFDAAVSGGL-NTSVLRAVLPRDMEFRTSTPRVVL
LCA         TREASREYEDKVWDKYGWLCKMHTGIVRDKKKK----E-----ITPHCALMDCIIFESASKARLPDLKTVHNILPHDLIFRGPNVVT-L
LCE         SKEASREYEDKVWDKYGWLCKMHTGVVRDKKKK----E-----ITPHCALMDCIIFESASKARLPDLPTVHNILPHDLIFRGPNVVT-L
MOP         QKDDARKFEDKIWDEYKHLCRMHTGIVTQKKKRGGKEE-----VTPHCALLDCLMFEAAVIGSP-QIPTPRPVLSRDLVFRTGPPRVVL
CD1         TSEQARQFDQQVWEKFGHLCKHHNGVVVSKKKRDKDAPFKLASSEPHCALLDCIMFQSVLDGKL-YEEELTPLLPPSLLFLPKAAYA-L
MC2         TSEQARQFDQQVWEKFGHLCKHHNGVVVSKKKRDKDAPFKLASSEPHCALLDCIMFQSVLDGKL-YEEELTPLLPPSLLFLPKAAYA-L
MAC         TSDQARLYDQQIWEKFGHLCKHHNGVVVNKKKREKDSPFKLSSGEPHCALLDCIMYQSVMDGKM-VDEEPVALLPLSLLFLPKAAFA-L
OLI         PTDQARFYESVVWEKFGSLCTKHNGVVLSRKKKGGNSG------EPHCALLDCLMFQAAFEGNV-PSIEPKPLLPSALVFKSESVVA-M
PIC         SAEQARTFEDEIWERYNQLCTKHKGLVIKKKKKKGAVQT----TANPPCALLDTIMFDATVTGWV-RDQKPMRCLPIDTLYRNNTDLINL
SAB         ASEQARKFEEPIWSDFGHLCKKHNGVIVPKKKKDKDIP---QSSEPHCALLDCLMFQSAIAGQP-PQTKLEGLLPDALLFTLEAAFT-I
TAC         TSDQARLFEHQVWDKFGHLCKQHNGVIISKKNKSKDSPPSPSPDEPHCALLDCIMFHSAVSGEL-PKEEPIPLLPKEFLFFPKTAFA-L
                497 500                           525   530
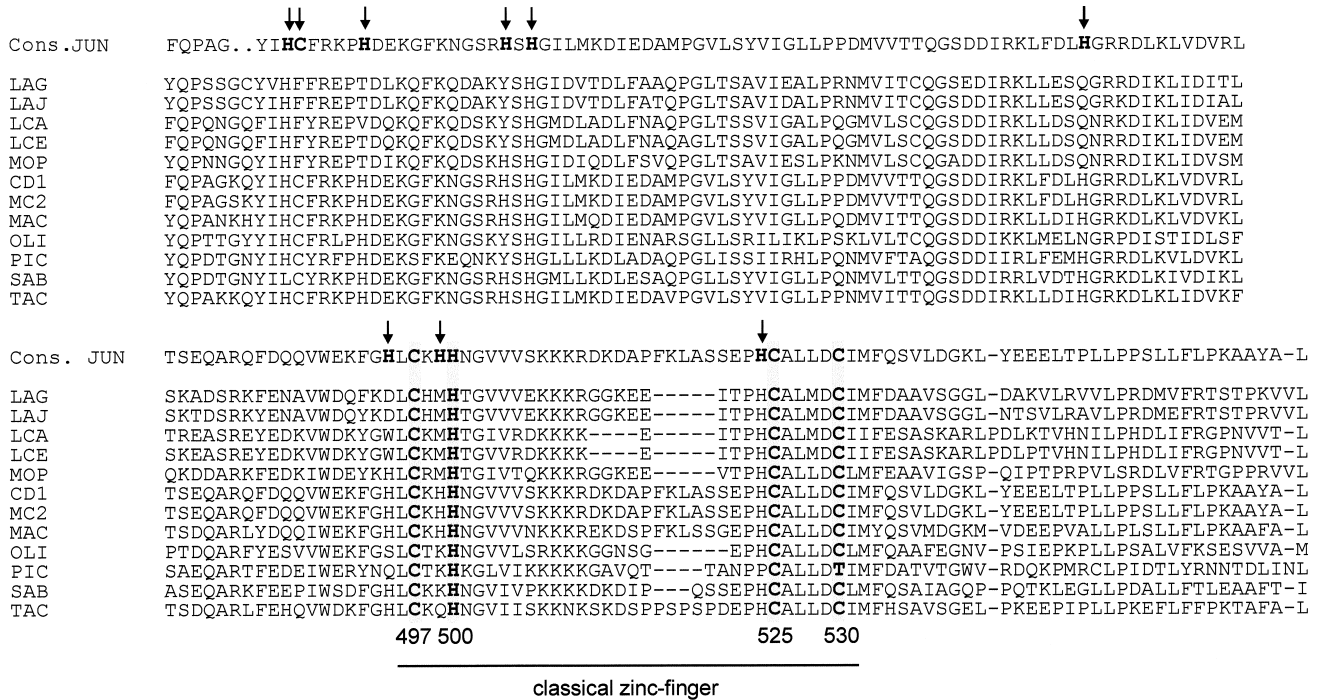```

_____
classical zinc-finger

**Fig. 1.** Multiple sequence alignment of the arenavirus nucleocapsid protein. The alignment was done using the Clustal X program. Gaps were included to maximize alignment of the homologous amino acids. The sequence $C_{497}H_{500}C_{525}C_{530}$ represents the amino acids involved in zinc-coordination in a zinc finger-like domain (shadowed). The numbers represent the amino acid positions in the N protein sequence of Junín virus. Arrows indicate positions of alternative amino acid residues that could coordinate zinc. Abbreviations: LAG, Lassa-Nigeria; LAJ, Lassa-Josiah; LCA, LCM-Armstrong; LCE, LCM-WE; MOP, Mopeia; CD1, Junín-Candid #1; MC2, Junín-MC2; MAC, Machupo; OLI, Oliveros; PIC, Pichindé; SAB, Sabiá; TAC, Tacaribe.

Horton *et al.*, 1990). In addition, carboxy-terminal deletions were introduced in the N ORF containing the point mutations using N1 primer plus ZfD(C497A; H500N)V and N1 plus ZfD(C530A)V (see Table 1). The N gene containing four amino acid substitutions in the full-length N ORF was used as a template. The ST1/ST2 heteroduplex was ligated to the amplified fragments. The mutant genes were finally generated by PCR using primers N1 and ST2 and were inserted into the *Nde*I site of pET-22b(+) vector. All these constructs were designed to express the heterologous protein starting from its own methionine codon and with no fused sequences at its carboxy terminus.

■ **DNA sequencing.** The identity of mutants was confirmed by sequencing via the chain-termination method (Sanger *et al.*, 1977) using the *fmol* DNA Sequencing System (Promega).

■ **Protein expression.** *E. coli* BL21(DE3) cells were transformed with recombinant plasmids, and recombinant cells were cloned. Protein expression was routinely induced with 1 mM IPTG for 4 h. *E. coli* cells were collected by centrifugation, rinsed with PBS, resuspended in 50 mM Tris–HCl pH 8·0, 100 mM NaCl, 1 mM EDTA, 0·5% Nonidet P-40 plus 0·2 mM PMSF and disrupted by sonication. After centrifugation, the recombinant proteins were collected from the insoluble fraction and analysed by SDS–PAGE (Laemmli, 1970).

■ **Immunoblotting.** Samples of bacterial extracts were separated by SDS–PAGE (10–20% gradient polyacrylamide gel), blotted onto nitrocellulose membranes (Schleicher & Schuell), and probed with a 1/100 dilution of human antiserum specific for Junín virus. Filters were then incubated with a goat anti-human antibody conjugated to alkaline phosphatase (Sigma) and developed using the chromogenic substrates NBT–BCIP (Promega).

■ **Zinc-binding.** The zinc-binding assay was carried out basically as described by Keck *et al.* (1993) with some modifications. Briefly, after electrophoresis equivalent gels were either stained with Coomassie brilliant blue or transferred to nitrocellulose membranes. The transferred proteins were renatured on the membranes by incubation at room temperature for 1 h in buffer A (100 mM Tris–HCl pH 7·5, 50 mM NaCl, 1 mM dithiothreitol). The membranes were briefly washed in the metal binding buffer (100 mM Tris–HCl pH 7·5, 50 mM NaCl) and probed for 1 h with 15 μM $^{65}$ZnCl$_2$ (3·12 mCi/mg; NEN Dupont) in the same buffer. The membranes were then washed twice over a 30 min period in buffer A. In competition experiments, divalent metal ions (10 mM) were included in the metal binding buffer during the incubation with $^{65}$ZnCl$_2$. Finally, nitrocellulose membranes were wrapped in Saran Wrap and autoradiographed using Kodak X-Omat film.

## Results

### Zinc-binding activity of the N protein *in vitro*

As shown in Fig. 1, a region with the potential to form a classical zinc-finger motif was found in the N protein amino acid sequence: $CX_2HX_{23}CX_4C$ (residues 497–530) (Parisi *et al.*, 1996).

In order to test the zinc-binding activity of the N protein, the N gene was expressed in *E. coli*. The proteins from a gel similar to the one in Fig. 2(A), were transferred to a nitrocellulose membrane, allowed to renature and probed with
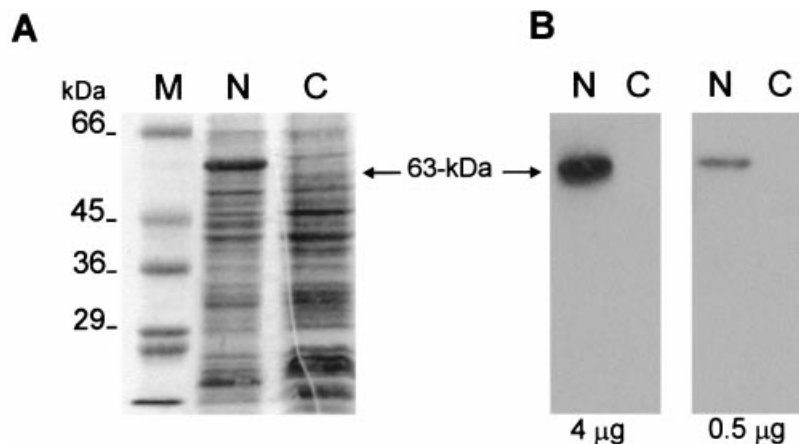
Fig. 2. Expression of the N gene of Junín virus in bacteria and zinc-binding activity of the encoded protein. *E. coli* transformed with the pET-N (lanes N) or with pET with no insert (lanes C) were induced with IPTG for protein expression. Proteins of total bacterial lysates were separated by SDS–polyacrylamide gel (10%) electrophoresis and stained with Coomassie brilliant blue (A), or transferred to nitrocellulose membrane and probed with $^{65}Zn^{2+}$ (B). The corresponding autoradiographs are shown. M, molecular mass marker (sizes in kDa indicated on the left).
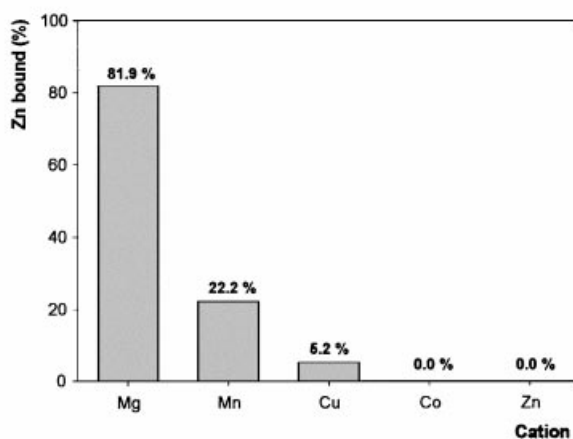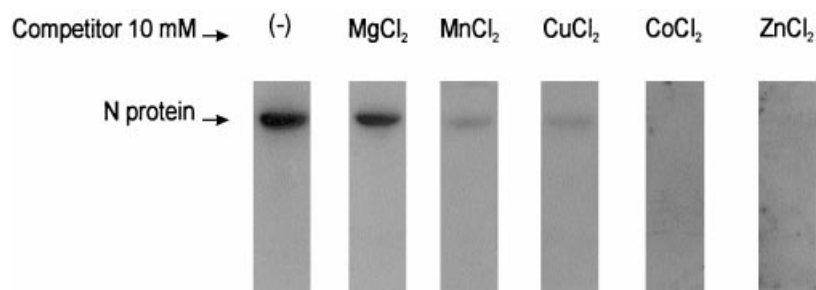


Fig. 3. Specificity of zinc-binding. A lysate of *E. coli* containing the 63 kDa N protein was applied to a polyacrylamide gel as in Fig. 2 (A). After electrophoresis the proteins were transferred to a membrane as in Fig. 2 (B). Individual strips were incubated with $^{65}Zn^{2+}$ in the presence of 10 mM $ZnCl_2$, $MgCl_2$, $MnCl_2$, $CoCl_2$, $CuCl_2$ or a control with no divalent metal ion. The membranes were then washed and autoradiographed. The radioactivity was quantified by densitometry; the results are expressed as % relative to the zinc bound in the absence of competitor. The membranes probed in the presence of $CoCl_2$ and $ZnCl_2$ were overexposed and demonstrate that there is no $^{65}Zn^{2+}$ binding.

$^{65}Zn^{2+}$. The results showed that the 63-kDa protein encoded by the N ORF had zinc-binding activity (Fig. 2B).

To further characterize the metal-binding properties of the N protein, competition experiments were done to determine the specificity of the zinc-binding activity. Identical samples obtained from lysates of *E. coli* expressing the 63 kDa protein were loaded onto equivalent lanes of a polyacrylamide gel, electrophoresed and blotted onto a membrane. After transfer, the membrane was cut into equivalent strips, each representing one lane, and probed with 15 μM $^{65}Zn^{2+}$ in the presence or absence of unlabelled competitor metal ions. The results showed in Fig. 3 indicate that the competition efficiency was $Zn^{2+} \cong Co^{2+} > Cu^{2+} > Mn^{2+} > Mg^{2+}$.

## The carboxy-terminal region of the N protein binds zinc *in vitro*

The predicted zinc-finger domain of the N protein $CX_2HX_{23}CX_4C$ is located in the carboxy-terminal region, comprising amino acid residues 497 to 530. To determine whether this region of the 63 kDa protein binds zinc, an artificial gene encoding the zinc-finger domain was made by PCR. Carboxy-terminal deletion variants of N lacking the zinc-finger domain were also generated. The amplified products were inserted into pET-22b(+). The heterologous proteins were expressed in *E. coli*, recovered from the insoluble fraction and separated on a triplicate set of 10–20% gradient
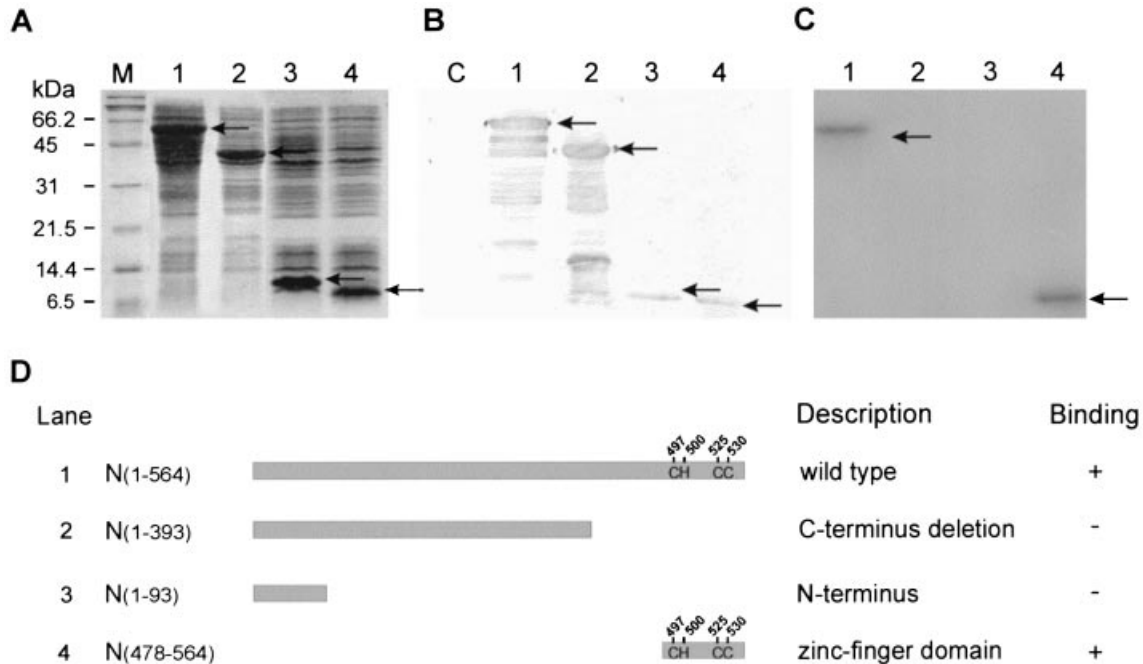
**Fig. 4.** Zinc binding by truncated N proteins. pET-22b(+) constructs containing the full-length N(1–564) and N(478–564) genes or truncated forms of N ORFs were expressed in *E. coli* and analysed by electrophoresis on an SDS–polyacrylamide gradient gel (10–20%). Gels were stained with Coomassie brilliant blue (A), blotted and probed with a Junín virus-specific antibody (B), or blotted and probed with $^{65}Zn^{2+}$ (C). Truncated variants of N are identified by the positions of the amino- and carboxy-terminal amino acid residues indicated in parentheses. The full-length protein is designated N(1–564); the truncated forms of the N protein are designated N(1–393) and N(1–93) and the protein with the putative zinc-finger domain is designated N(478–564) (lanes 1, 2, 3 and 4, respectively). The horizontal grey bars represent the N-derived polypeptides. Cysteine and histidine residues in the predicted zinc-finger motif are indicated by C and H. The relative zinc-binding capacities of the proteins are summarized on the right (D).

polyacrylamide gels; one of them was stained with Coomassie brilliant blue (Fig. 4 A), and the others transferred to nitrocellulose membranes. One of the transferred membranes was probed with a Junín virus-specific polyclonal antibody (Fig. 4 B) and the other was probed with $^{65}Zn^{2+}$. Only the N(478–564) protein retained the ability to bind $^{65}Zn^{2+}$ (Fig. 4 C). Therefore, we inferred that the last 86 amino acids, comprising the zinc-finger motif (amino acids 497–530), are sufficient to bind zinc *in vitro* (Figs 1 and 4 D).

### The carboxy-terminal region of the N protein has alternative residues that bind zinc *in vitro*

To establish whether the zinc-binding activity was due to the classical zinc-finger motif, point mutations were made by PCR in the full-length N(1–564) and in the N(478–564) ORFs. Each cysteine of the motif ($CX_2HX_{23}CX_4C$) was changed to alanine (C → A) and the histidine residue was changed to asparagine (H → N). The PCR products containing these point mutations were inserted into pET-22b(+) and expressed in *E. coli*. The approximate masses of the wild-type or mutant N(1–564) and N(478–564) proteins were determined by SDS–PAGE and Coomassie brilliant blue staining (Fig. 5 A). Then, similar molar amounts of these proteins were applied onto an SDS–polyacrylamide gel, transferred to a nitrocellulose membrane and probed with $^{65}Zn^{2+}$. As shown in Fig. 4 (C), no zinc-binding activity was detected in the truncated mutants N(1–393) and N(1–93) (Fig. 5 B, lanes 5 and 6, respectively). When all four residues were changed in the N(478–564) protein, no zinc-binding activity was detected (Fig. 5 B, compare lanes 7 and 8). Thus, the zinc-finger motif, located between amino acids 497 and 530, appears to be both necessary and sufficient for binding zinc.

Nevertheless, the zinc-binding activity was not abolished when these same four amino acid residues were changed in the full-length N protein N(1–564) quadruple mutant protein (Fig. 5 B, lane 2). This unexpected result required an additional analysis, since the region immediately adjacent to the zinc-finger domain was not included in the series of truncated mutants used in Fig. 4. To verify if this region was also involved in zinc binding, we expressed two additional truncated proteins, designated N(1–536) quadruple mutant and N(1–502) double mutant, which also included the point mutations that abolished the zinc-binding activity of the N(478–564) quadruple mutant. Interestingly, both of these mutants bound zinc *in vitro* (Fig. 5 B, lanes 3 and 4, respectively). These data indicate that amino acid residues between positions
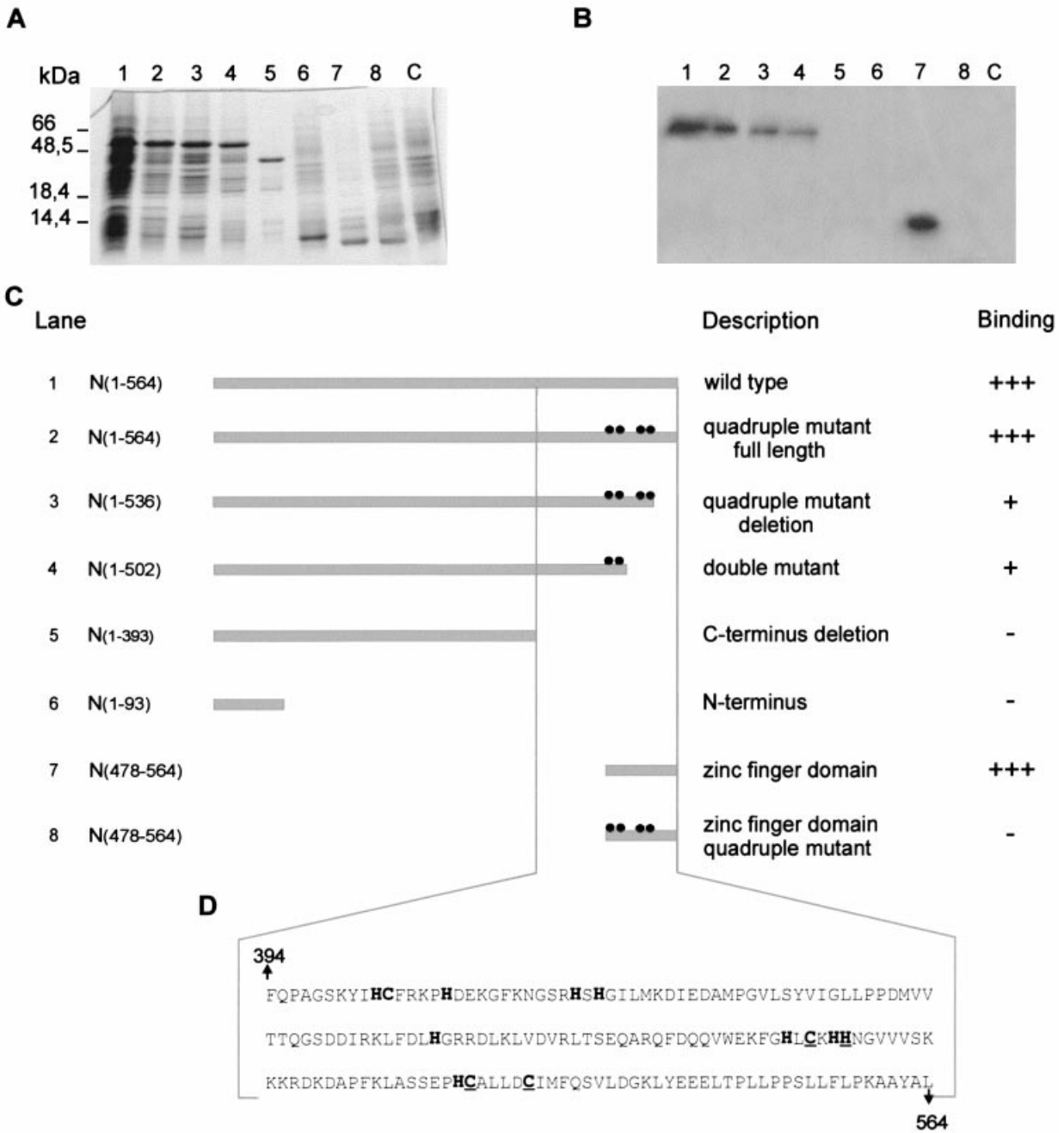
**A**



**B**

**C**

| Lane | | | Description | Binding |
|------|---|---|-------------|---------|
| 1 | N(1-564) | | wild type | +++ |
| 2 | N(1-564) | •• •• | quadruple mutant full length | +++ |
| 3 | N(1-536) | •• •• | quadruple mutant deletion | + |
| 4 | N(1-502) | •• | double mutant | + |
| 5 | N(1-393) | | C-terminus deletion | – |
| 6 | N(1-93) | | N-terminus | – |
| 7 | N(478-564) | | zinc finger domain | +++ |
| 8 | N(478-564) | •• •• | zinc finger domain quadruple mutant | – |

**D**

394
↑
FQPAGSKYI**HC**FRKP**H**DEKGFKNGSR**H**S**H**GILMKDIEDAMPGVLSYVIGLLPPDMVV

TTQGSDDIRKLFDL**H**GRRDLKLVDVRLTSEQARQFDQQVWEKFG**H**L**C**K**HH**NGVVVSK

KKRDKDAPFKLASSEP**HC**ALLD**C**IMFQSVLDGKLYEEELTPLLPPSLLFLPKAAYAL
↓
564

**Fig. 5.** Zinc blot analysis of N mutant proteins. Mutant proteins were analysed by electrophoresis on an SDS–polyacrylamide gradient gel (10–20%) and stained with Coomassie brilliant blue (A). A duplicate gel was transferred to a nitrocellulose membrane and probed with $^{65}Zn^{2+}$ (B). The relative zinc-binding abilities are summarized on the right. Cysteine-to-alanine mutations and histidine-to-asparagine mutations are indicated above the bars with dots (C). (D) N protein sequence of the region responsible for the zinc-binding activity: the amino acids that could be involved in zinc-coordination are indicated in bold and the amino acids involved in the zinc-finger domain are underlined.

394 and 502 can also be involved in zinc binding and explain the results observed with the N(1–564) quadruple mutant. In accordance with these results, this region has several potential coordination sites which could be involved in zinc coordination (Fig. 5 D).

## Discussion

The evidence presented here documents the zinc-binding capacity of the N protein of Junín virus and describes the metal ion-binding specificity. In experiments designed to characterize

the zinc-binding properties of the Z protein, Salvato & Shimomaye (1989) noted that the N protein of lymphocytic choriomeningitis virus (LCMV) binds zinc *in vitro*. In accordance with their results, we found a zinc-finger motif conserved at the carboxy-terminal region of all arenavirus N proteins (Parisi *et al.*, 1996). The classical zinc-finger motif is characterized by two conserved cysteines and histidines which bind to a zinc ion in a tetrahedral coordination, thereby stabilizing a structure that comprises an antiparallel two-stranded $\beta$-sheet and an $\alpha$-helix. The amino-terminal end of the $\alpha$-helix is responsible for establishing DNA or RNA sequence-specific interactions (Nolte *et al.*, 1998; McColl *et al.*, 1999). Other classes of zinc fingers have been described which differ from the classical zinc finger in the metal ion-binding motif, the number of coordinated zinc ions, or the structure of the sequence-specific nucleic acid-binding region. The most frequent of these motifs is the so-called 'RING finger', characterized by the presence of two zinc-binding domains. In the general RING motif, each zinc atom is ligated tetrahedrally by either four cysteines, or three cysteines and a histidine. One of these RING fingers was described in the Z protein of LCMV (Lovering *et al.*, 1993). As shown in Fig. 1, Junín virus nucleocapsid protein has the sequence $CX_2HX_{23}CX_4C$ (positions 497, 500, 525 and 530), which resembles a classical zinc-binding motif and is well conserved among arenaviruses (Parisi *et al.*, 1996). At this point, it is important to note that the N protein of Pichindé virus does not contain the cysteine-525; instead, there is a threonine residue which could potentially form a hydrogen bond with a water molecule that may also coordinate zinc (Coleman, 1992). In line with these considerations, the complete N protein of Junín virus expressed in bacteria displays zinc-binding activity *in vitro* (Fig. 2B). Assessment of the metal-binding specificity of the N protein was done by competition experiments. In these experiments, N protein was probed with $^{65}Zn^{+2}$ in the presence or absence of unlabelled competitor metal ions. The competitor efficiency was $Zn^{2+} \cong Co^{2+} > Cu^{2+} > Mn^{2+} > Mg^{2+}$ (Fig. 3). These results are consistent with a specific zinc-binding activity and are similar to data obtained with the protein encoded by the vaccinia virus A2L gene (Keck *et al.*, 1993). *A priori*, many amino acid residues in the N sequence could coordinate $Zn^{2+}$ in addition to the $CX_2HX_{23}CX_4C$ motif. To determine if the N protein region containing the putative zinc-finger was responsible for zinc binding we made a series of deletion mutants. The results indicate that the location of the zinc-binding activity is coincident with the putative zinc-finger region (Fig. 4). To establish if the zinc-binding activity was due to the putative zinc-finger motif, we made a series of point mutants. When the four amino acids predicted as critical in the zinc finger were mutated in the N(478–564) protein, the zinc-binding capacity was abolished (Fig. 5B, lane 8). However, when the same four mutations were introduced into the full-length N protein, only a slight decrease in zinc-binding capacity was apparent (Fig. 5B, lane 2). These results suggest an

alternative zinc-coordination site (or sites) in the region immediately adjacent to or partially overlapping with the classical zinc-finger domain. This amino acid sequence comprises eight histidines and a cysteine, in addition to those that participate in the classical zinc finger, that could be involved in alternative zinc binding. Some of these amino acids are conserved in the *Arenaviridae* (Fig. 1). According to this, the truncated N(1–502) mutant containing the indicated point mutations should interact with zinc, as shown in Fig. 5, lane 4. This combined mutant comprises the N(1–393) protein region plus 109 amino acids (not represented in any of the previously analysed deletion mutants) and only half of the predicted zinc-finger domain in which both amino acids involved in the characterized zinc-finger activity were substituted. The smaller amount of zinc bound to mutant proteins N(1–536) and N(1–502), relative to full-length N, might be the reflection of a change in the structure and/or the stability of the alternative zinc-coordination site(s) due to the lack of the carboxy-terminal region (Fig. 5B, lanes 3 and 4 compared to lane 2). In support of these speculations several reports indicate that different degrees of change in the folding of a series of proteins are due to very limited alterations at their carboxy termini (Orellano *et al.*, 1993; Clérico *et al.*, 2000; Derman & Agard, 2000). The complete zinc-binding domain of N might adopt one of a number of different structures. It is also possible that the N protein has two independent binding sites: the classical zinc finger and the region immediately adjacent to it. However, our experiments do not rule out the possibility that these two binding sites exclude one another or bind zinc simultaneously, acting as a unique RING-finger-like structure. Further experiments should address the relevance of these residues in zinc binding and the significance of the zinc-binding activity in the N protein interactions that lead to the formation of nucleocapsids and/or to the transcriptional antitermination activity (Tortorici *et al.*, 2000).

# References

**Albariño, C. G., Ghiringhelli, P. D., Posik, D. M., Lozano, M. E., Ambrosio, A. M., Sanchez, A. & Romanowski, V. (1997).** Molecular characterization of attenuated Junín virus strains. *Journal of General Virology* **78**, 1605–1610.

**Albariño, C. G., Posik, D. M., Ghiringhelli, P. D., Lozano, M. E. & Romanowski, V. (1998).** Arenavirus phylogeny: a new insight. *Virus Genes* **16**, 39–46.

**Auperin, D., Romanowski, V., Galinski, M. S. & Bishop, D. H. L. (1984).** Sequencing studies of Pichindé arenavirus S RNA indicate a novel coding strategy, an ambisense viral S RNA. *Journal of Virology* **52**, 897–904.

**Clérico, E. M., Peisajovich, S. G., Ceolín, M., Ghiringhelli, P. D. & Ermácora, M. R. (2000).** Engineering a compact non-native state of intestinal fatty acid-binding protein. *Biochimica et Biophysica Acta* **1476**, 203–218.

**Coleman, J. E. (1992).** Zinc proteins: enzymes, storage proteins, transcription factors, and replication proteins. *Annual Review of Biochemistry* **61**, 897–946.

**Derman, A. I. & Agard, D. A. (2000).** Two energetically disparate folding pathways of alpha-lytic protease share a single transition state. *Nature Structural Biology* **7**, 394–397.

**Franze-Fernández, M. T., Iapalucci, S., Lopez, N. & Rossi, C. (1993).** Subgenomic RNAs of Tacaribe virus. In *The Arenaviridae*, pp. 113–132. Edited by M. S. Salvato. New York: Plenum Press.

**Ghiringhelli, P. D., Rivera Pomar, R. V., Lozano, M. E., Grau, O. & Romanowski, V. (1991).** Molecular organization of Junín virus S RNA: complete nucleotide sequence, relationship with the other members of Arenaviridae and unusual secondary structures. *Journal of General Virology* **72**, 2129–2141.

**Ghiringhelli, P. D., Albariño, C. G., Piboul, M. & Romanowski, V. (1997).** The glycoprotein precursor gene of the attenuated Junin virus vaccine strain (Candid#1). *American Journal of Tropical Medicine and Hygiene* **56**, 216–225.

**Higuchi, R. (1989).** In *PCR technology. Principles and Applications for DNA Amplification*, pp. 61–70. Edited by H. A. Erlich. New York: Stockton Press.

**Horton, R. M., Cai, Z. L., Ho, S. N. & Pease, L. R. (1990).** Gene splicing by overlap extension: tailor-made genes using the polymerase chain reaction. *Biotechniques* **8**, 528–535.

**Keck, J. G., Feigenbaum, F. & Moss, B. (1993).** Mutational analysis of a predicted zinc-binding motif in the 26-kilodalton protein encoded by the vaccinia virus A2L gene: correlation of zinc-binding with late transcriptional transactivation activity. *Journal of Virology* **67**, 5749–5753.

**Laemmli, U. K. (1970).** Cleavage of structural proteins during the assembly of the head of bacteriophage T4. *Nature* **227**, 680–685.

**Lee, K. J., Novella, I. S., Teng, M. N., Oldstone, M. B. A. & de la Torre, J. C. (2000).** NP and L proteins of lymphocytic choriomeningitis virus (LCMV) are sufficient for efficient transcription and replication of LCMV genomic RNA analogs. *Journal of Virology* **74**, 3470–3477.

**Lovering, R., Hanson, I. M., Borden, K. L. B., Martin, S., O'Reilly, N. J., Evan, G. I., Rahman, D., Pappin, D. J. C., Trowsdale, J. & Freemont, P. S. (1993).** Identification and preliminary characterization of a protein motif related to the zinc finger. *Proceedings of the National Academy of Sciences, USA* **90**, 2112–2116.

**McColl, D. J., Honchell, C. D. & Frankel, A. D. (1999).** Structure-based design of an RNA-binding zinc finger. *Proceedings of the National Academy of Sciences, USA* **96**, 9521–9526.

**Nolte, R. T., Conlin, R. M., Harrison, S. C. & Brown, R. S. (1998).** Differing roles for zinc fingers in DNA recognition: structure of a six-finger transcription factor IIIA complex. *Proceedings of the National Academy of Sciences, USA* **95**, 2938–2943.

**Orellano, E. G., Calcaterra, N. B., Carrillo, N. & Ceccarelli, E. A. (1993).** Probing the role of the carboxyl-terminal region of ferredoxin–NADP$^+$ reductase by site-directed mutagenesis and deletion analysis. *Journal of Biological Chemistry* **268**, 19267–19273.

**Parisi, G., Echave, J., Ghiringhelli, P. D. & Romanowski, V. (1996).** Computational characterization of potential RNA-binding sites in arenavirus nucleocapsid proteins. *Virus Genes* **13**, 249–256.

**Romanowski, V. (1993).** Genetic organization of Junín virus, the etiological agent of Argentine hemorrhagic fever. In *The Arenaviridae*, pp. 51–83. Edited by M. S. Salvato. New York: Plenum Press.

**Salvato, M. S. & Shimomaye, E. M. (1989).** The completed sequence of lymphocytic choriomeningitis virus reveals a unique RNA structure and a gene for a zinc finger protein. *Virology* **173**, 1–10.

**Sambrook, J., Fritsch, E. F. & Maniatis, T. (1989).** *Molecular Cloning: A Laboratory Manual*, 2nd edn. Cold Spring Harbor, NY: Cold Spring Harbor Laboratory.

**Sanger, F., Nicklen, S. & Coulson, A. R. (1977).** DNA sequencing with chain-terminating inhibitors. *Proceedings of the National Academy of Sciences, USA* **74**, 5463–5467.

**Thompson, J. D., Gibson, T. J., Plewniak, F., Jeanmougin, F. & Higgins, D. G. (1997).** The Clustal X windows interface: flexible strategies for multiple sequence alignment aided by quality analysis tools. *Nucleic Acids Research* **25**, 4876–4882.

**Tortorici, M. A., Albariño, C. G., Posik, D. P., Ghiringhelli, P. D., Lozano, M. E., Rivera Pomar, R. & Romanowski, V. (2000).** Arenavirus nucleocapsid protein displays a transcriptional antitermination activity *in vivo*. *Virus Research* (in press).